Multi-wall carbon nanostructured paper: characterization and potential applications definition

Yamila M Omar[1], **Carlo Maragliano**[1], **Chia-Yun Lai**[1], **Francesco Lo Iacono**[1,2], **Nicolas Bologna**[1,2], **Maria Vittoria Diamanti**[2], **Tushar Shah**[3], **Amal Al Ghaferi**[1] **and Matteo Chiesa**[1]

[1] Institute Center for Energy (iEnergy), Masdar Institute of Science and Technology, Abu Dhabi, United Arab Emirates
[2] Dipartimento di Chimica, Materiali ed Ingegneria Chimica 'G. Natta', Politecnico di Milano, Milano, Italy
[3] Applied Nanostructured Solutions, LLC, 2323 Eastern Boulevard, Baltimore, MD 21220, USA

E-mail: aalghaferi@masdar.ac.ae **and** mchiesa@masdar.ac.ae

Keywords: carbon materials, carbon nanotubes, electrical properties, energy storage, surface properties, wetting

Supplementary material for this article is available online

RECEIVED
12 May 2015

REVISED
13 July 2015

ACCEPTED FOR PUBLICATION
31 July 2015

PUBLISHED
7 September 2015

1. Introduction

Carbon is a versatile element that allows for zero-, one-, two- and three-dimensional materials with very broad properties. Engineered nanostructures such as fullerenes, carbon nanotubes (CNT) and graphene have extraordinary properties when compared with traditional three-dimensional samples such as graphite and diamond. For example, in terms of electrical properties, while a C_{60} (0D) crystal is insulating just like pure diamond (3D) [1], metallic single wall carbon nanotubes (SWNT) (1D) exhibit ballistic transport of electrons with long mean free paths (in the order of microns), and semiconductor SWNTs and MWNTs (1D) show characteristics of diffusive transport [2] that lead to conductivity values three to four orders of magnitude higher than graphite (3D). Graphene, the 2D single layer of graphite, has in turn the best electrical conductivity of all, when measured in plane [1].

The specific surface area (SSA) of carbon-based materials is also quite variable between different nanostructures. Theoretical values for CNTs show that the SSA decreases as the number of walls and the diameter of the nanotube increases [3], allowing for a broad span of values from 50 to 1315 $m^2 g^{-1}$. In the case of graphene, theoretical calculations predict a value of SSA as high as 2630 $m^2 g^{-1}$ if both sides of the 2D sheet are considered [3]. These nanostructured materials can potentially achieve very high SSA when compared to graphite experimental values, which range from 61 to 104 $m^2 g^{-1}$ depending on the adsorbed vapor [4]. Furthermore, since the energy stored in an electric double layer (EDL) is related to the capacitance ($E = CV^2/2$) which is in turn dependent on the surface area ($= {}_r\epsilon\epsilon_0 CA/$) [5*d*] of the active mass, the specific capacitance of different carbon nanostructured materials is expected to vary in the same way as their surface area.

Wetting is among the least variable of properties with all pristine carbon based materials showing some degree of hydrophobic behavior (graphite, $\theta \approx 90^o$ [6]; buckypaper made of CNT, $\theta \approx 113$–120^o [7, 8]; graphene on copper, $\theta \approx 85^o$ [9]; etc) and strong aging dependency of the wetting [6, 9]. Furthermore, it has been shown that water affinity can be modified by means of certain treatments, such as ultraviolet (UV) light and

ozone exposure [7], and the application of an electric field [10] to produce a transition from hydrophobic to hydrophilic or even super-hydrophilic wetting behavior. On the other hand, SCA measurements of organic liquids such as acetonitrile, propylene carbonate or 1-butyl-3-methylimidazolium (BMIMBF4), on carbon based materials have resulted in good wetting affinity ($\theta < 26^{o}$) [11, 12].

The main weakness of much of the literature presented so far is that these studies focus on characterizing and/or improving only one parameter at the time neglecting the interplay between different properties. In real applications, the optimization of multiple material properties is required in order to perform at the frontier of their field. In this work, a complete study of a new, low cost, easy to manufacture multi-wall carbon nanostrustured free-standing paper-like material (MWCNS-p) is conducted. The building blocks of our material, called MWCNS, are defined as highly entangled MWNTs that exhibit cross-linking and wall sharing (see supplementary information). This nanostructure is 3D in nature, since it is constructed of a three-dimensional CNT web with covalent bonds between junctions, leading to enhanced properties of its one-dimensional counterpart. Given the novelty of this nanostructured material and the multiple requirements of the potential applications discussed in this work, a holistic characterization of electrical, electrochemical, surface and water affinity properties is conducted to compare its performance against other carbon-based nanostructured materials.

2. Experimental

350 mg of long, highly oriented CNS (see supplementary information) produced by Lockheed Martin [13] were added to 2 L of 1:1 v/v mixture of ethanol/water. The suspension was sonicated and then vacuum filtrated through a fiberglass filter. The MWCNS dump formed was removed from the filter and dried in a convection oven at 80 °C. The final material is the MWCNS-p.

The sample was imaged using a Quanta 250 SEM and an Asylum Research MFP3D atomic force microscope (AFM), using Asylum Research AC240TS silicon tips. Cross section images were taken using a Quanta 3D focused ion beam dual beam SEM.

The electrical resistivity was measured with a 2-probe Hall machine from LockShore on van der Pauw specimens. Also traditional 4-probe in line measurements were done. CV and galvanostatic charge discharge were performed using an Autolab PGSTAT128N. A 9.5 mg electrode was submerged in a 1M NaCl/DI water solution. A niobium counter-electrode and a Ag/AgCl reference electrode (207.7 mV versus SHE) completed the set-up. The input current was 1 mA. The surface area was measured by means of BET using liquid nitrogen at 77 K, after degasing the sample in vacuum at 400 °C for 4 h.

The macroscopic static contact angle (SCA) of DI water droplets was measured with a DM-501 goniometer from Kyowa Interface Science Co. Ltd A Quanta 250 Environmental SEM (ESEM) was used to determine microscopic SCA. A 90° sample holder and system rotation of $\alpha = 5°$ were used. Water condensation was achieved at 760–800 Pa and 2 °C. The software developed by Stalder *et al* [14] and the mathematical method proposed by Brugnara and coworkers [15] to compensate for the non-perpendicular view line of the surface where the droplets are condensed were used to determine the SCA of ESEM condensed droplets.

Fourier transform infrared spectroscopy (FTIR) was conducted on MWCNS-p samples at 42 °C in nitrogen atmosphere while heating for 6 h. After this period of time, humidity was added and changes in the surface were evaluated for 6 more hours. Thermal stability of the sample was studied by means of Thermal Gravimetric Analysis on a TG 449 F3 Jupiter from NETZSCH coupled with a TGA-IR (FTIR) on a Vertex 80 V spectrometer form Bruker Optics. Nitrogen gas atmosphere was used and temperature ramps of 5 °C min^{-1} from 40 to 600 °C.

3. Results and discussion

3.1. Imaging

Figure 1(a) shows a SEM image of the surface of the MWCNS-p thin film, while figure 1(b) shows a tapping mode AFM image of a 0.25 μm^2 section. As it can be observed, the material appears to be an entangled web of CNTs and only at high magnifications branching is discernible. From figure 1(b), the CNS outer diameter was estimated to be in the order of 20–30 nm. The estimation assumes that the apparent width is, to a first approximation, $2R$ larger than the true diameter [16]. Here R is the effective tip radius which was established to be approximately 10 nm by means of the critical amplitude method [17, 18]. The cross section of the MWCNS-p in figure 1(c) shows no evident packing arrangement of the CNS. In addition, figures 1(a) and (b) were analyzed by means of two-dimensional fast Fourier transform (2D-FFT) to determine the orientation of the CNS. Results plotted in figure 1(d) indicate that the MWCNS-p are randomly oriented in opposition to the as-produced MWCNS powder (see supplementary information, figure S2).

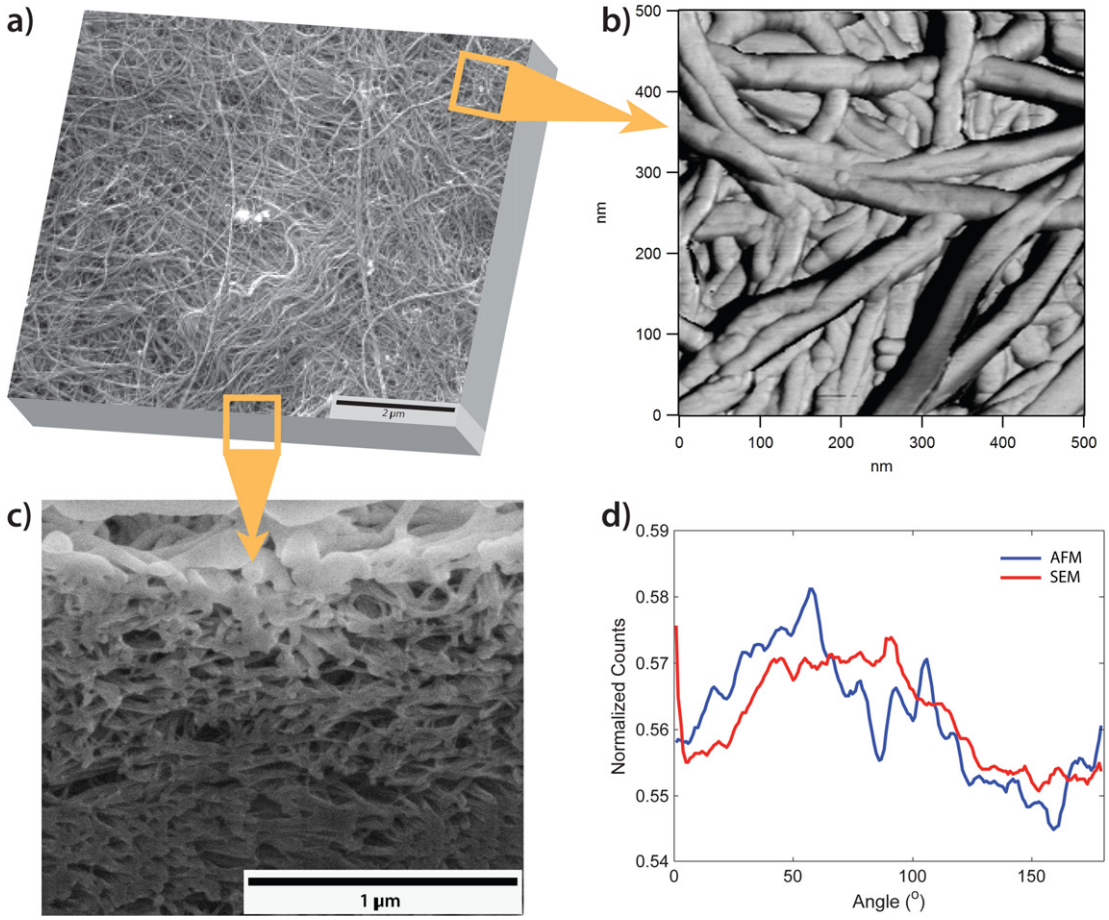

Figure 1. (a) SEM image of the MWCNS-p thin film. The bar indicates a scale of 2 μm. (b) Tapping mode AFM image. The diameter of the MWCNS was estimated to be 20–30 nm. (c) SEM image of the MWCNS-p cross section, (the bar indicates a scale of 1 μm). (d) 2D-FFT results of the images in (a) and (b) indicating that the MWCNS are oriented at random within the paper sample. The angle indicates the orientation angle of the MWCNS in the plane of the paper.

Table 1. Summary of multiwall carbon nanostructured paper properties.

Property	CNS-p paper
Electrical resistivity	5.8–13.8 mΩ cm
Electrical conductivity	72.5–172.4 S cm^{-1}
Surface area (BET)—raw material	253 m^2 g^{-1}
Surface area (BET)	149 m^2 g^{-1}
Specific capacitance (CV)	6.3 F g^{-1}
Specific capacitance (GCD)	43 F g^{-1}
Macroscopic static contact angle (SCA)	117° $\pm$ 3°
Microscopic static contact angle (ESEM)	130° $\pm$ 8°

3.2. Electrical characterization

Electrical characterization results are summarized in table 1. The values obtained from 2-probe and 4-probe measurements are essentially equal, only varying from $\sigma = 1/\rho \cong$ 72.5 to 172.4 s cm^{-1} for pristine and compressed (under 750 PSI) samples, respectively. When compared with other carbon-based materials, MWCNS-p paper electrical conductivity is in the same order of magnitude as that for CNT and graphene paper samples [19, 20] as indicated in figure 2. We note that typical IV curves to determine the electrical properties of the samples were also carried out with the use of conductive AFM. These experiments however proved to be cumbersome and imprecise given the high forces developed between tip and sample that lead to MWCNS being pulled out and we have therefore not reported the results here for lack of reproducibility.

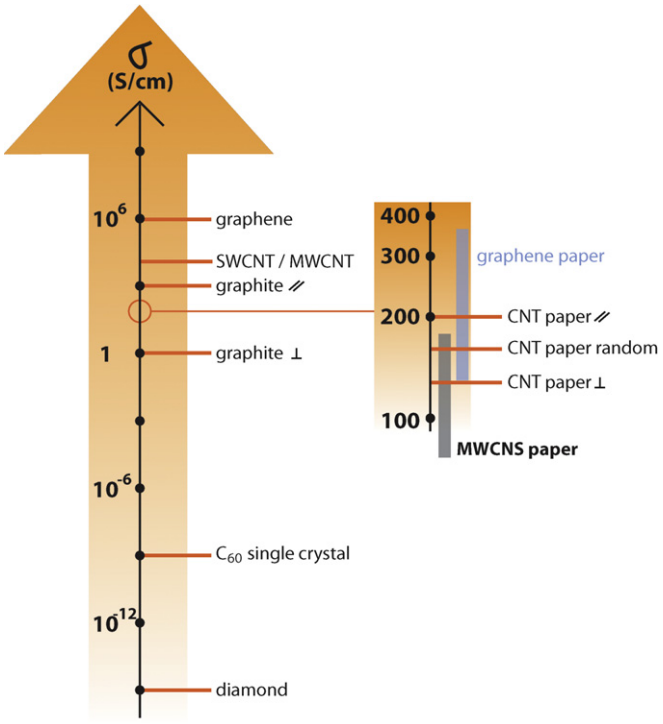

Figure 2. Comparison between different carbon-based materials electrical conductivity. It can be observed that MWCNS-p paper has σ values of the same order of magnitude as CNT and graphene paper [1, 19–22].

3.3. Electrochemical characterization

Figure 3(a) shows the results obtained by cyclic voltammetry (CV). Direct inspection of the figure shows that the cyclic voltammogram is nearly rectangular thus showing that the system behaves, to a first approximation, as an ideal capacitor [23]. Furthermore, the current increases steadily with the voltage (i.e. no peaks, and therefore, no faradaic reactions, are observed), and the charging and discharging of the electrodes is fast for all scan rates. Finally, the anodic and cathodic currents are increasing functions of the scan rate. These results lead us to conclude that ions are adsorbed on the surface of the electrode forming an EDL due to Coulombic interaction, and that no oxidation or reduction chemical reactions take place. This interpretation further allows us to quantify the specific capacitance of the electrode, thus facilitating comparison with other materials. Given the known relationship between the cyclic voltammogram loop area and the scan rate [24]

$$\int_{V_1}^{V_2} I(V)\mathrm{d}V = 2\Delta V m\ C\nu,$$

where ΔV is the voltage range used (0–0.7 V), m is the mass of the electrode (g), ν is the scan rate (mV s^{-1}) and C is the specific capacitance (F g^{-1}), the area of the loop $\int_{V_2}^{V_1} I(V)\mathrm{d}V$ was plotted versus the scan rate ν, allowing for the specific capacitance to be calculated from the slope k as $C = k/(2\Delta V m)$ giving a value of 6.3 F g^{-1}.

Figure 3(b) shows the galvanostatic charge-discharge (GCD) test performed on a MWCNS-p electrode. The specific capacitance of the electrode was calculated from the slope of the discharge curves using the equation [25]

$$C = \frac{2}{m}\frac{I}{(\mathrm{d}V/\mathrm{d}t)},$$

Where C is specific capacitance (F g^{-1}), m is the electrode mass (g), I is the input current (A) and $\mathrm{d}V/\mathrm{d}t$ is the slope of the discharge curve (V s^{-1}). The factor 2 indicates that the total capacitance measured is the addition of two equivalent single electrode capacitors connected in series [25]. The specific capacitance obtained by this method is 43 $\pm$ 7 F g^{-1}. This value is within the 4 to 87.5 F g^{-1} range of results obtained in literature [19, 25, 26] for MWNT capacitor electrodes tested by GCD. Further comparison of the specific capacitance of the MWCNS-p paper with other materials is show in figure 4 and discussed in the following section in relation with the material's surface area.

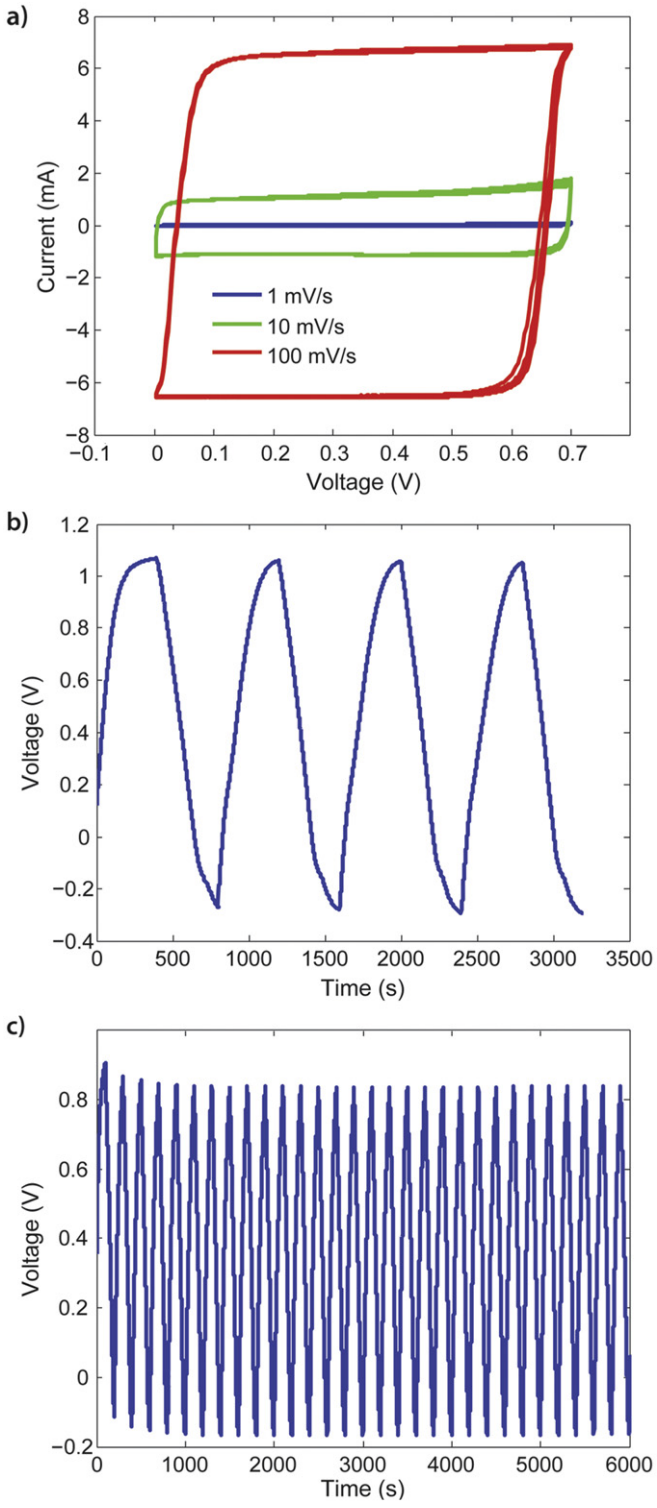

Figure 3. (a) Cyclic voltammogram of a MWCNS-p paper electrode in 1 M NaCl / DI water solution at 1, 10 and 100 mV s^{-1} scan rates. Ten curves were recorded for each scan rate showing no electrode degradation; (b) galvanostatic charge-discharge at a current input of 1 mA and a ramp of 400 s; (c) fast GCD indicating electrode stability over several cycles.

It is noted that CV and GCD tests do not render the same result for the specific capacity of the electrode. As explained elsewhere [23], galvanostatic measurements are considered more reliable than CV because the current is kept at a constant value and the time can be determined with accuracy, giving capacity values with accuracy better than 1%. On the other hand, CV suffers from time-dependent phenomena that may interfere with the measurement at high scan rates [23]. Therefore, it is recommended to use slow scan rates in order for electrochemical processes to occur sufficiently fast when compared with the scan rate if an accurate value of the specific capacity is to be determined. Thus, the value of the specific capacitance obtained by GCD will be used to compare our MWCNS-p electrode with other electrode materials (see figure 4).

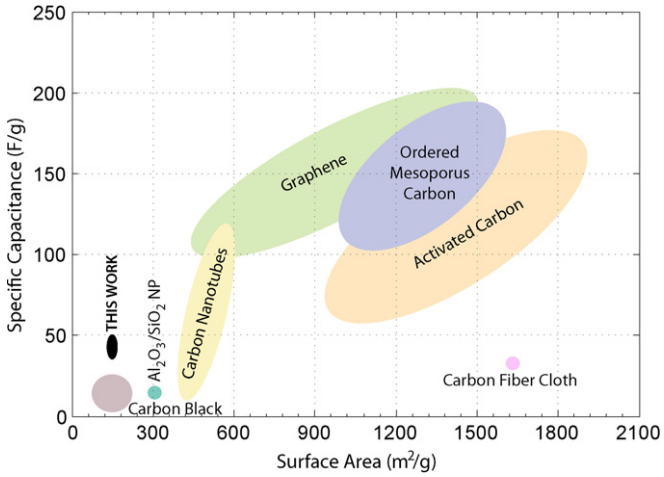

Figure 4. Comparison of MWCNS paper specific capacitance and surface area with other materials used for electrodes in energy storage applications [29, 30].

Finally, the electrodes stability was proved by repeating CV and confirmed by fast and continuous cycling using GCD. Results of the latter are illustrated in figure 3(c), where it can be observed that the electrodes showed no degradation during repetitive cycling.

3.4. Surface area and pore structure

The surface areas of the raw material and the MWCNS-p paper measured by BET were 253 and 149 $m^2\ g^{-1}$ respectively (table 1). It is noteworthy that the value obtained for the MWCNS powder is in excellent agreement with that theoretically predicted for MWNTs by Peigney *et al* [3] (see supplementary information). The lower surface area of the free-standing paper sample can be explained by the much more compact structure in comparison with the powder. In addition, it was estimated from BET results that 90% of mesopore diameters in the thin film were in the range between 3 and 8 nm (see supplementary information, figure S3), in agreement with literature [27].

As explained in the introduction, an increase in surface area would moderately improve the specific capacitance of the sample. However, it is fair to argument the very high cost-to-benefit ratio: costly and cumbersome techniques, such as low temperature chemical fusion [28] of a precursor to form a porous partially carbonized film on the CNS, are required. Nevertheless, the specific capacitance of $43 \pm 7\ F\ g^{-1}$ obtained by GCD is rather low when compared with other materials [29, 30] used as active masses in batteries or supercapacitors (figure 4). This value can be enhanced by addition of metal oxides that undergo fast surface redox (pseudo-capacitive) reactions such as ruthenium (RuO_2) and manganese (MnO_2) oxides [31] disregarding the value of the surface area.

3.5. Water affinity

The SCA of ambient exposed samples led to the expected hydrophobic behavior of carbon-derived materials, $\theta = 117^\circ \pm 3^\circ$ (figure 5(a)). The SCA of droplets condensed within an ESEM yielded, as expected, slightly higher values of $\theta = 130^\circ \pm 8^\circ$ (figure 5(b)).

Carbon derived materials exposed to atmospheric conditions adsorb small amounts of contaminants from the environment until equilibrium conditions are met [9, 32]. Adsorbed species change the electrical [33–35] properties and wettability [32] of samples. The adsorbed layer of water vapor on the surface of MWCNS-p after long exposure to controlled humidity [33] or ambient conditions [36] reported by previous studies was confirmed here by means of FTIR as shown in figure 5(c). Curves were obtained for the MWCNS-p membrane during heating at 42 °C for 6 h in nitrogen atmosphere showing water desorption. Exposure to water vapor for 6 h proved insufficient time to reach initial conditions (figure 5(c)). TGA measurements conducted in nitrogen atmosphere detected a 0.3% of weight loss at temperatures up to 100 °C (data not shown). We attribute this mass loss to desorbed water due to ambient exposure as indicated by FTIR measurements. However, infrared (IR) analysis of the exhaust gases did not detect the O–H vibration mode of water, possibly due to low partial pressure of water in the exhaust gas mixture (data not shown).

The pristine sample was baked in a vacuum oven at 120 °C for 12 h, after which the SCA was measured obtaining super-hydrophobic behavior ($\theta > 140^o$). The sample was aged in ambient conditions presenting a SCA $> 135^o$ for 72 h indicating slow water adsorption kinetics (figure 5(d)). After this period of time, the aged

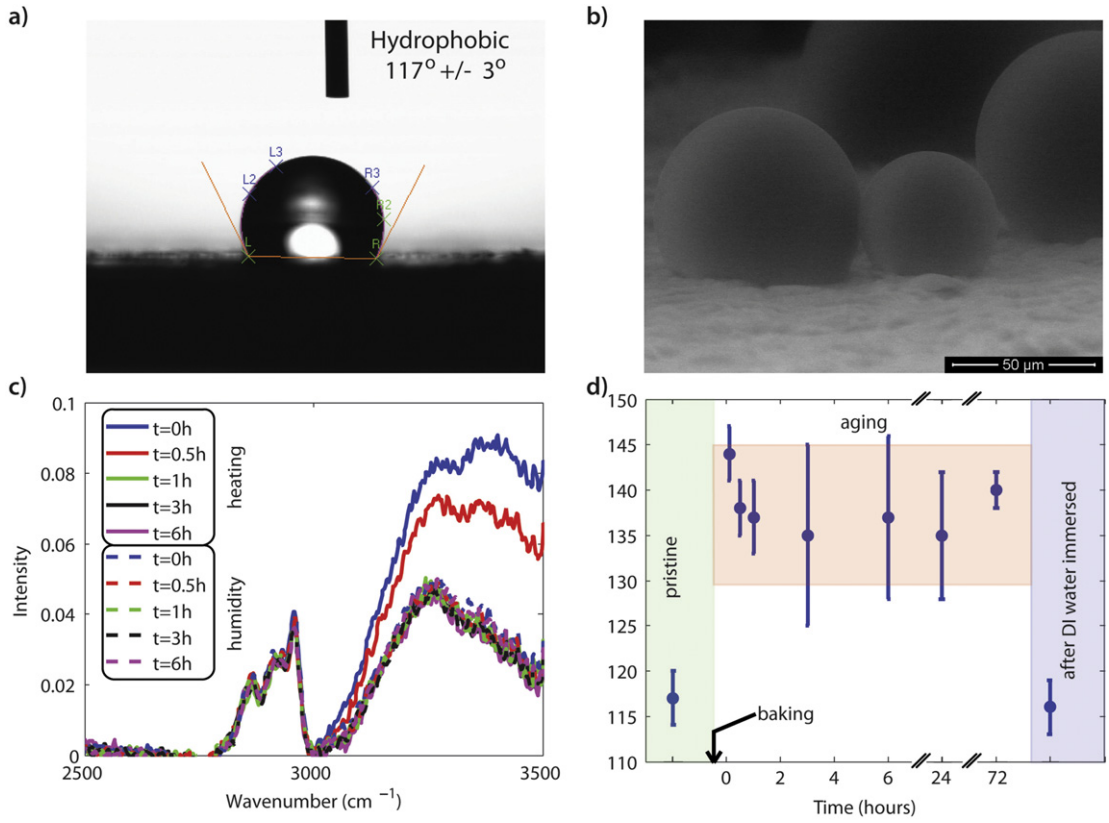

Figure 5. (a) Macroscopic SCA of ambient exposed MWCNS paper; (b) ESEM image of water vapor condensation on the MWCNS paper surface; (c) Fourier transform infrared spectroscopy of a sample baked at 42 °C in nitrogen atmosphere (full line curves) for 6 h and then exposed to humidity for 6 h (dash line curves). Slow water adsorption kinetics lead to no difference between FTIR curves during 6 h of humidity exposure; and (d) static contact angle of the pristine sample, the baked sample at different aging times and the baked sample after immersion in DI water. Again, water adsorption kinetics is slow, giving no change in SCA in 3 days. However, the wetting behavior of the pristine sample is recovered after immersion in DI water.

sample was immersed in DI water and allowed to dry in air. The wetting behavior was now equivalent to that of the pristine sample. These results show that, like for graphene and graphite [6, 9], the MWCNS-p hydrophobic behavior is modified when water is adsorbed on its surface. Specifically, for the MWCNS-p the hydrophobic behavior is reduced, something that is desirable in applications where an aqueous electrolyte is used in contact with the electrode material [37]. It is noteworthy, that organic electrolytes will have better wetting affinity in contact with carbon based samples. Preliminary SCA measurements of organic liquids, such as decane, castor oil and isopropanol on atomically flat highly ordered pyrolytic graphite have shown complete spreading (see supplementary information, figure S4). Although this means that the effective surface area contributing to the creation of the EDL will be much higher for organic liquids than in the case of aqueous electrolytes, the measured specific capacitance is not expected to increase due to the lower relative dielectric constant of organic liquids in comparison to water.

3.6. Potential applications

Excellent electrical conductivity and moderate specific capacitance indicate that MWCNS-p is adequate for energy storage applications that rely on the formation of an EDL in the interface between the active mass and the electrolyte, like batteries [38], supercapacitors [5] and fuel cells [38]. As discussed in previous sections, it is recommended to combine the MWCNS-p with pseudo-capacitive oxides to enhance its specific capacitance. Furthermore, surface treatment to improve the water wetting behavior is highly recommended to better the contact between the active mass and the electrolyte [37]. This is of particular interest if, for example, the application of MWCNS-p is intended for capacitive deionization (CDI) [39], a technique that allows for the removal of deleterious ions from a stream of water by applying an electric field between two electrodes and trapping the ions in the EDL developed in the electrode/electrolyte interface. It is noteworthy that energy storage devices and CDI cells are a great examples of potential applications with multiple material properties requirements where high electrical conductivity, large surface area, high specific capacitance and excellent water affinity are required simultaneously.

4. Conclusions

In summary, we have presented a holistic characterization of the electrical, electrochemical, surface and wetting properties of a low cost, easy to manufacture MWCNS free-standing paper. We interpreted our results in light of other carbon-based nanostructured materials and analyzed the MWCNS-p potential to be used as electrode for energy storage devices that rely on the formation of an EDL to store energy, such as batteries and supercapacitors, or for example, in CDI where the formation of an EDL is used to separate solvated ions from a water stream with the aim of producing drinking water. All these applications require simultaneous optimization of multiple parameters, vindicating the necessity of a holistic characterization of MWCNS-p material properties. Furthermore, it can be concluded that properties such as high electrical conductivity, moderate surface area and hydrophobic wetting behavior of the 1D counterpart (MWNTs) are retained within the three-dimensional cross-linked web of MWCNS.

Acknowledgments

This work was supported by Applied Nanostructure Solutions grant to the Laboratory of Energy and Nanosciences (LENS) in Masdar Institute. The authors would like to thank Dr Guanqiu Li for his constant assistance and predisposition, Maritsa Kissamitaki for artwork assistance and Harry Apostoleris for proofreading the manuscript.

References

[1] Delhaes P 2013 *Carbon Based Solids and Materials* (New York: Wiley)
[2] Bachtold A *et al* 2000 Scanned probe microscopy of electronic transport in carbon nanotubes *Phys. Rev. Lett.* **84** 6082
[3] Peigney A *et al* 2001 Specific surface area of carbon nanotubes and bundles of carbon nanotubes *Carbon* **39** 507–14
[4] Broadbent K, Dollimore D and Dollimore J 1966 The surface area of graphite calculated from adsorption isotherms and heats of wetting experiments *Carbon* **4** 281–7
[5] Simon P and Gogotsi Y 2008 Materials for electrochemical capacitors *Nat. Mater.* **7** 845–54
[6] Amadei C A *et al* 2014 Time dependent wettability of graphite upon ambient exposure: the role of water adsorption *J. Chem. Phys.* **141** 084709
[7] Dumee L *et al* 2011 Enhanced durability and hydrophobicity of carbon nanotube bucky paper membranes in membrane distillation J. *Membr. Sci.* **376** 241–6
[8] Dumée L F *et al* 2010 Characterization and evaluation of carbon nanotube bucky-paper membranes for direct contact membrane distillation *J. Membr. Sci.* **351** 36–43
[9] Lai C-Y *et al* 2014 A Nanoscopic approach to studying evolution in graphene wettability *Carbon* **80** 784–92
[10] Kakade B *et al* 2008 Electric field induced, superhydrophobic to superhydrophilic switching in multiwalled carbon nanotube papers *Nano Lett.* **8** 2693–6
[11] Debgupta J, Kakade B A and Pillai V K 2011 Competitive wetting of acetonitrile and dichloromethane in comparison to that of water on functionalized carbon nanotube surfaces *Phys. Chem. Chem. Phys.* **13** 14668–74
[12] Zhou C and Kumar S 2006 Comparison of carbon nanotube based electrochemical supercapacitor electrodes using different electrolytes *Polymer Preprints* **47** 376
[13] Malet B K and Shah T K 2014 Glass substrates having carbon nanotubes grown thereon and methods for production thereof *US Patent* US 8784937 B2
[14] Stalder A *et al* 2006 A snake-based approach to accurate determination of both contact points and contact angles *Colloids and Surf.* A **286** 92–103
[15] Brugnara M *et al* 2006 Contact angle analysis on polymethylmethacrylate and commercial wax by using an environmental scanning electron microscope *Scanning* **28** 267–73
[16] Bustamante C and Keller D 2008 Scanning force microscopy in biology *Phys. Today* **48** 32–8
[17] Sergio Santos L G, Sourier T, Gadelrab K and Chiesa M 2012 A method to provide rapid in situ determination of tip radius in dynamic atomic force microscopy *Rev. Sci. Instrum.* **83** 043707
[18] Maragliano C *et al* 2015 Effective AFM cantilever tip size: methods for *in-situ* determination *Meas. Sci. Technol.* **26** 015002
[19] Wang D *et al* 2008 Highly oriented carbon nanotube papers made of aligned carbon nanotubes *Nanotechnology* **19** 075609
[20] Chen H *et al* 2008 Mechanically strong, electrically conductive, and biocompatible graphene paper *Adv. Mater.* **20** 3557–61
[21] Wen C *et al* 1992 Electrical conductivity of a pure C60 single crystal *Appl. Phys. Lett.* **61** 2162–3
[22] Souier T *et al* 2013 How to achieve high electrical conductivity in aligned carbon nanotube polymer composites *Carbon* **64** 150–7
[23] Béguin F and Frackowiak E 2010 *Carbons for Electrochemical Energy Storage and Conversion Systems* (Boca Raton, FL: CRC Press)
[24] Chen W *et al* 2010 Enhanced capacitance of manganese oxide via confinement inside carbon nanotubes *Chem. Commun.* **46** 3905–7
[25] Shaijumon M *et al* 2008 Synthesis of hybrid nanowire arrays and their application as high power supercapacitor electrodes *Chem. Commun.* **2008** 2373–5
[26] Frackowiak E *et al* 2000 Supercapacitor electrodes from multiwalled carbon nanotubes *Appl. Phys. Lett.* **77** 2421–3
[27] Smajda R *et al* 2007 Structure and gas permeability of multi-wall carbon nanotube buckypapers *Carbon* **45** 1176–84
[28] Liu Y *et al* 2013 Synthesis of porous carbon nanotubes foam composites with a high accessible surface area and tunable porosity J. *Mater. Chem.* A **1** 9508–16
[29] AlMarzooqi F A *et al* 2014 Application of capacitive deionisation in water desalination: a review *Desalination* **342** 3–15
[30] Yu A, Chabot V and Zhang J 2013 *Electrochemical Supercapacitors for Energy Storage and Delivery: Fundamentals and Applications* (Boca Raton, FL: CRC Press)
[31] Lee S W *et al* 2010 Carbon nanotube/manganese oxide ultrathin film electrodes for electrochemical capacitors *Acs Nano* **4** 3889–96

[32] Amadei C A *et al* 2013 The aging of a surface and the evolution of conservative and dissipative nanoscale interactions *J. Chem. Phys.* **139** 084708
[33] Zahab A *et al* 2000 Water-vapor effect on the electrical conductivity of a single-walled carbon nanotube mat *Phys. Rev.*B **62** 10000
[34] Kong J *et al* 2000 Nanotube molecular wires as chemical sensors *Science* **287** 622–5
[35] Collins P G *et al* 2000 Extreme oxygen sensitivity of electronic properties of carbon nanotubes *Science* **287** 1801–4
[36] Whitten P G, Spinks G M and Wallace G G 2005 Mechanical properties of carbon nanotube paper in ionic liquid and aqueous electrolytes *Carbon* **43** 1891–6
[37] Porada S *et al* 2013 Review on the science and technology of water desalination by capacitive deionization *Prog. Mater. Sci.* **58** 1388–442
[38] Winter M and Brodd R J 2004 What are batteries, fuel cells, and supercapacitors? *Chem. Rev.* **104** 4245–70
[39] Anderson M A, Cudero A L and Palma J 2010 Capacitive deionization as an electrochemical means of saving energy and delivering clean water comparison to present desalination practices: Will it compete? *Electrochim. Acta* **55** 3845–56